

Measurements of time-dependent CP violation in B -meson decays at LHCb

Stefano Perazzini^{a,*}

^a*INFN, Sezione di Bologna, Italy*

E-mail: stefano.perazzini@bo.infn.it

Studying the CP violation originating from the interference between the mixing and the decay processes of neutral B mesons is an excellent instrument to investigate the presence of physics beyond the Standard Model. In this paper the most recent measurements of time-dependent CP violation in $B_{(s)}^0$ decays performed by the LHCb collaboration are presented. The measurements are conducted using proton-proton collisions data recorded with the LHCb detector during the Run1 and Run2 of the LHC. The determination of the CKM phase difference $\gamma - 2\beta_s$ using a sample of $B_s^0 \rightarrow D_s^- K^+ \pi^+ \pi^-$ decays is shown, as well as the first observation of time-dependent CP violation in the B_s^0 sector using a sample of $B_s^0 \rightarrow K^+ K^-$ decays.

BEAUTY2020

21-24 September 2020

Kashiwa, Japan (online)

*Speaker, on behalf of LHCb collaboration

1. Introduction

Time-dependent CP violation in neutral B-meson decays originates from the interference between two processes: the $B_{(s)}^0$ - $\bar{B}_{(s)}^0$ mixing, *i.e.* the transformation of $B_{(s)}^0$ mesons from their particle to their antiparticle states (and *vice versa*), and the decay. The amplitudes of the diagrams responsible for these processes depend on the values of the elements of the Cabibbo-Kobayashi-Maskawa (CKM) matrix [1], which models CP violation in charged-current quark transitions in the Standard Model (SM). Precise measurements of the time-dependent CP asymmetries of $B_{(s)}^0$ decays constrain the values of the CKM matrix elements, representing a validity test of the SM itself. In addition, since the mixing process is governed by second-order diagrams, new particles, not included in the SM, may appear inside the loops as virtual contributions, altering the observed CP asymmetries with respect to their SM predictions.

When a $B_{(s)}^0$ meson can decay to both the final state f and to its charge conjugate \bar{f} two distinct CP asymmetries as a function of the decay time are observed, depending on the final state:

$$\begin{aligned} A_{CP}^f(t) &= \frac{-C_f \cos(\Delta m_{d(s)}t) + S_f \sin(\Delta m_{d(s)}t)}{\cosh\left(\frac{\Delta\Gamma_{d(s)}}{2}t\right) + A_f^{\Delta\Gamma} \sinh\left(\frac{\Delta\Gamma_{d(s)}}{2}t\right)}, \\ A_{CP}^{\bar{f}}(t) &= \frac{-C_f \cos(\Delta m_{d(s)}t) - S_f \sin(\Delta m_{d(s)}t)}{\cosh\left(\frac{\Delta\Gamma_{d(s)}}{2}t\right) + A_{\bar{f}}^{\Delta\Gamma} \sinh\left(\frac{\Delta\Gamma_{d(s)}}{2}t\right)}, \end{aligned} \quad (1)$$

where $\Delta m_{d(s)}$ and $\Delta\Gamma_{d(s)}$ are the mass and width differences of the mass eigenstates of the $B_{(s)}^0$ system. When the final state f is a CP eigenstate, it implies $f \equiv \bar{f}$, hence $S_f \equiv -S_{\bar{f}}$ and $A_f^{\Delta\Gamma} \equiv A_{\bar{f}}^{\Delta\Gamma}$ and the two asymmetries in Eq. (1) become a single one. In the case of flavour-specific decays $C_f = 1$ and $S_f = S_{\bar{f}} = A_f^{\Delta\Gamma} = A_{\bar{f}}^{\Delta\Gamma} = 0$, but is possible to define the time-integrated CP asymmetry $A_{CP} = (|\bar{A}_{\bar{f}}|^2 - |A_f|^2) / (|\bar{A}_{\bar{f}}|^2 + |A_f|^2)$ between the squares of the amplitudes of the decays $B \rightarrow f$ (A_f) and $\bar{B} \rightarrow \bar{f}$ ($A_{\bar{f}}$).

In this paper we present time-dependent measurements using samples of $B_s^0 \rightarrow D_s^- h^+ \pi^+ \pi^-$ decays ($h = K, \pi$) [2], as well as the measurement of time-dependent and time-integrated CP asymmetries in the decays of $B_{(s)}^0$ mesons to charged two-body final states with kaons and pions (namely $B^0 \rightarrow \pi^+ \pi^-$, $B_s^0 \rightarrow K^+ K^-$, $B^0 \rightarrow K^+ \pi^-$ and $B_s^0 \rightarrow \pi^+ K^-$) [3].¹ The former analysis is conducted using proton-proton (p - p) collision data collected with the LHCb detector at centre-of-mass energies of 7, 8 (Run 1 data) and 13 TeV (Run 2 data) and corresponding to an integrated luminosity of 9 fb^{-1} . The latter analysis is performed using a partial sample of p - p collision data collected during the Run 2 and corresponding to an integrated luminosity of 1.9 fb^{-1} .

Common ingredients of the two analyses are: the determination of the flavour of the $B_{(s)}^0$ meson at production (flavour tagging) and the calibration of the decay-time resolution, both diluting the amplitude of the observed time-dependent asymmetry; the determination of the decay-time efficiency, that sculpts the decay-time distribution of selected decays; the determination of the asymmetries between the selection efficiency of charge-conjugate final states (detection asymmetry) and between the production rates of $B_{(s)}^0$ and $\bar{B}_{(s)}^0$ mesons (production asymmetry). The flavour tagging is performed by analysing either the decay products of the other beauty hadron in the

¹Unless stated otherwise, the inclusion of charge-conjugate decay modes is implied throughout this document.

event (opposite-side or OS tagging), or the products of the hadronisation process of the signal $B_{(s)}^0$ meson (same-side or SS tagging) [4]. The calibration is performed using flavour-specific decays whose observed time-dependent asymmetry is proportional to the dilution factor introduced by the probability of assigning a wrong initial flavour to the signal (mistag probability). The decay-time resolution is calibrated by measuring the width of the decay-time distribution of decays reconstructed using particles originating directly in the primary p - p collision vertex (PV). The efficiency as a function of the decay time is determined using decays topologically similar to the signals and having a well measured lifetime. The production asymmetry is determined using flavour-specific decays with the method explained in Ref. [5]. The detection asymmetry is dominated by the different cross section of K^+ and K^- with the detector material and is measured using $D^+ \rightarrow K^- \pi^+ \pi^+$ and $D^+ \rightarrow K_s^0 \pi^+$ decays according to Ref. [6]. An additional contribution is due to different efficiencies of the particle identification (PID) criteria when applied to positively and negatively charged particles. This contribution is corrected using a calibration sample of $D^{*+} \rightarrow D^0(K^- \pi^+) \pi^+$ decays.

2. Measurement of the CKM angle γ and B_s^0 - \bar{B}_s^0 mixing frequency with $B_s^0 \rightarrow D_s^- h^+ \pi^+ \pi^-$ decays

The $B_s^0 \rightarrow D_s^- K^+ \pi^+ \pi^-$ decay is dominated by the tree-level transitions $b \rightarrow c$ and $b \rightarrow u$, and the interference between these transitions and B_s^0 - \bar{B}_s^0 mixing makes the CP -violation coefficients S_f , $S_{\bar{f}}$, $A_f^{\Delta\Gamma}$ and $A_{\bar{f}}^{\Delta\Gamma}$ sensitive to the difference between CKM phases $\gamma - 2\beta_s$ [7], where $\gamma \equiv \arg[-(V_{ud}V_{ub}^*)/(V_{cd}V_{cb}^*)]$ and $-2\beta_s$ is the B_s^0 mixing phase. The signal candidates are reconstructed combining D_s^- mesons (decaying to $K^- K^+ \pi^-$, $K^- \pi^+ \pi^-$ and $\pi^- \pi^+ \pi^-$ final states) with three additional charged tracks to form a B_s^0 vertex. PID requirements are used to distinguish between pions and kaons. The B_s^0 candidates are further selected using a boosted decision tree (BDT) in order to suppress the combinatorial background. The residual background components are subtracted by means of the $sPlot$ technique [8] using the invariant mass as discriminating variable. A background-subtracted sample of $B_s^0 \rightarrow D_s^- \pi^+ \pi^- \pi^+$ decays, selected in the same way, is used to calibrate the per-event mistag probability, and also to determine the shape of the decay-time efficiency. The flavour tagging reduces the effective statistics of the sample to $(5.71 \pm 0.40)\%$ and to $(6.52 \pm 0.17)\%$ of the total for the Run1 and Run2 samples, respectively. These efficiencies are very good considering the hard environment in p - p collisions. Candidates with the same topology as the signal, but with all the final-state tracks originating from the PV, are used to calibrate the per-event decay-time error obtaining an average resolution of 36.6 ± 0.5 fs and a decay-time bias of -2 fs. In order to take into account the variation of the strong phase entering the CP -violation coefficients across the phase space of the decay, a flavour-tagged time-dependent amplitude analysis of the $B_s^0 \rightarrow D_s^- K^+ \pi^+ \pi^-$ decay is performed. An alternative and model-independent method is also used, integrating the flavour-tagged decay-time distribution of the signal over the phase space. In exchange for a great simplification of the analysis, a dilution factor that reduces the sensitivity to $\gamma - 2\beta_s$ is introduced by this integration. Unbinned maximum-likelihood fits to the background-subtracted flavour-tagged decay-time distribution of the signal and control sample are performed. From the control sample the most precise determination of the B_s^0 mixing frequency to date is obtained $\Delta m_s = (17.757 \pm 0.007 \pm 0.008) \text{ ps}^{-1}$, where the first uncertainty is statistical and the second systematic. The dominant systematic uncertainty is due to the decay-time bias. The

model-dependent analysis of the signal determines directly the value of $\gamma - 2\beta_s$, while the model-independent analysis first determines the CP-violation coefficients of Eq.(1) and then combines them to obtain $\gamma - 2\beta_s$. The model-dependent and model-independent results are

$$\begin{aligned}(\gamma - 2\beta_s)_{\text{M.D.}} &= 42 \pm 10 \pm 4 \pm 5, \\(\gamma - 2\beta_s)_{\text{M.I.}} &= 42_{-13}^{+19+6}_{-2},\end{aligned}$$

respectively. The first uncertainties are statistical and the second systematic, while the third uncertainty for the model-dependent result is due to the alternative amplitude models considered. The dominant systematic uncertainties for the model-independent analysis are due to the background subtraction and to the calibration of decay-time resolution. Both determinations of $\gamma - 2\beta_s$ are in agreement with each other and with the world-average value [9, 10].

3. Observation of CP violation in two-body $B_{(s)}^0$ -meson decays to charged pions and kaons

The CP asymmetries of two-body $B_{(s)}^0$ mesons decays to charged pions and kaons are sensitive to the CKM angles γ and α , and to the B^0 and B_s^0 mixing phases, 2β and $-2\beta_s$. In addition, these decays have the potential to reveal physics beyond the SM, since they receive relevant contributions from $b \rightarrow s$ and $b \rightarrow d$ penguin diagrams [11]. Pairs of oppositely-charged tracks are combined to form signal candidates that are then separated into $\pi^+\pi^-$, K^+K^- and $K^+\pi^-$ final-state samples using PID requirements. A BDT is used to reduce the combinatorial background, retaining most of the signal. Two different experimental techniques are used to measure the CP-violating coefficients for the $B^0 \rightarrow \pi^+\pi^-$ and $B_s^0 \rightarrow K^+K^-$. The first method (simultaneous method) adapts a fitting model similar to that described in Ref. [12], describing all the components contributing to the samples, to all the final state simultaneously. This method also measures the time-integrated CP asymmetries of the $B^0 \rightarrow K^+\pi^-$ and $B_s^0 \rightarrow \pi^+K^-$ decays. The second method (per-candidate method) performs separate fits to the flavour-tagged decay-time distributions of $B^0 \rightarrow \pi^+\pi^-$ and $B_s^0 \rightarrow K^+K^-$ decays, where the background components are subtracted using the *sPlot* technique. Both methods use the $B^0 \rightarrow K^+\pi^-$ decays and a sample of $B_s^0 \rightarrow D_s^-\pi^+$ decays to calibrate the flavour tagging. The effective statistics is reduced by the flavour tagging to $(4.5 \pm 0.2)\%$ and to $(5.1 \pm 0.2)\%$ of the total for the $B^0 \rightarrow \pi^+\pi^-$ and $B_s^0 \rightarrow K^+K^-$ decays, respectively. The decay-time resolution is calibrated using $J/\psi \rightarrow \mu^+\mu^-$ and $\Upsilon(1S) \rightarrow \mu^+\mu^-$ decays originating from the PV. The simultaneous method uses an average decay-time resolution of 43.5 ps, while the second method uses a per-candidate calibration that returns the same averaged resolution. A decay-time bias of -6 fs is observed due to detector misalignments. An additional difference between the two methods is in the determination of the decay-time efficiency. The simultaneous method calibrates this using the $B^0 \rightarrow K^+\pi^-$ decays, while the per-event method determines the efficiency on a per-candidate basis using the *swimming* technique [13]. In Fig. 1, the observed time-dependent asymmetries for the $B^0 \rightarrow \pi^+\pi^-$ and $B_s^0 \rightarrow K^+K^-$ decays are shown. The compatibility between the two results is tested using pseudoexperiments and, including the uncorrelated systematic uncertainties, they are found to be compatible within one standard deviation. The systematic uncertainties are dominated by the calibration of the decay-time resolution and the decay-time efficiency for the $B_s^0 \rightarrow K^+K^-$

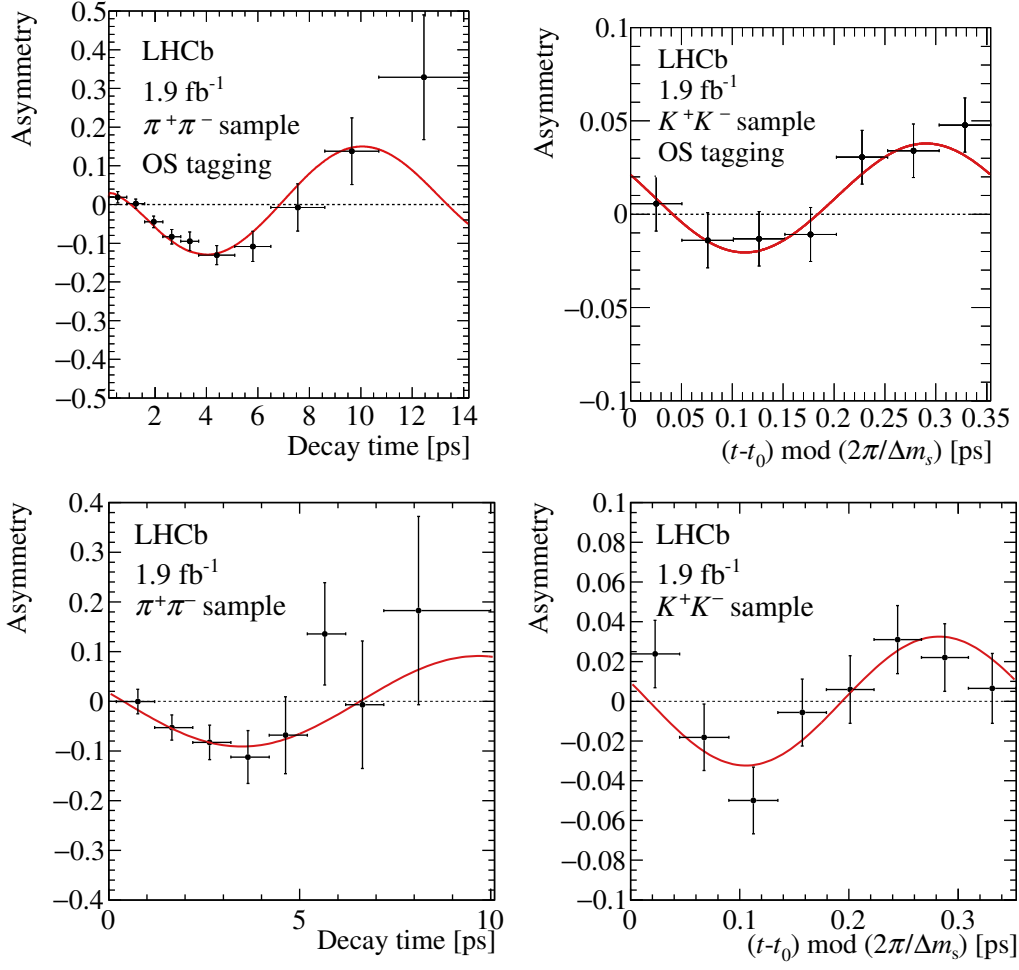


Figure 1: Time-dependent asymmetries for (top left) $\pi^+\pi^-$ candidates with $5.20 < m(\pi^+\pi^-) < 5.35 \text{ GeV}/c^2$, (top right) K^+K^- candidates with $5.30 < m(K^+K^-) < 5.44 \text{ GeV}/c^2$, (bottom left) background-subtracted $B^0 \rightarrow \pi^+\pi^-$ candidates and (bottom right) background-subtracted $B_s^0 \rightarrow K^+K^-$ candidates. In the top plots the asymmetry is obtained using only the OS-tagging information, while in the bottom the OS- and SS-tagging information is combined. The results of the simultaneous and per event fits are overlaid onto the data points in the top and bottom plots, respectively. The asymmetries for the K^+K^- candidates are folded into one mixing period $2\pi/\Delta m_s$ and the parameter $t_0 = 0.2 \text{ ps}$ corresponds to the minimum value of the decay-time used in the fit.

decay, the modelling of signal and background components for the $B^0 \rightarrow \pi^+\pi^-$ decay, and the determination of the detection asymmetry for the time-integrated CP asymmetries of the $B^0 \rightarrow K^+\pi^-$ and $B_s^0 \rightarrow \pi^+K^-$ decays. The LHCb results are quoted for the simultaneous method since this method has a slightly smaller total uncertainty and, measuring also the direct CP asymmetries, allow a complete combination with the previous LHCb measurements [12]. The results of the

combination are

$$\begin{aligned}
C_{\pi\pi} &= -0.320 \pm 0.038, \\
S_{\pi\pi} &= -0.672 \pm 0.034, \\
A_{CP}^{B^0} &= -0.0831 \pm 0.0034, \\
A_{CP}^{B_s^0} &= 0.225 \pm 0.012, \\
C_{KK} &= 0.172 \pm 0.031, \\
S_{KK} &= 0.139 \pm 0.032, \\
\mathcal{A}_{KK}^{\Delta\Gamma} &= -0.897 \pm 0.087,
\end{aligned}$$

representing the most precise determination of these quantities to date and are in agreement with the measurements performed by other experiments. According to a χ^2 test statistics, the values of the CP-violation coefficients of the $B_s^0 \rightarrow K^+K^-$ decay are incompatible with CP conservation with a significance exceeding 6 standard deviations. This represents the first observation of time-dependent CP asymmetry in the decays of the B_s^0 meson.

References

- [1] N. Cabibbo, *Phys. Rev. Lett.* **10** (1963) 531; M. Kobayashi and T. Maskawa, *Prog. Theor. Phys.* **49** (1973) 652
- [2] LHCb collaboration, R. Aaij *et al.*, [arXiv:2011.12041](https://arxiv.org/abs/2011.12041).
- [3] LHCb collaboration, R. Aaij *et al.*, *JHEP* **03** (2021) 75.
- [4] LHCb collaboration, R. Aaij *et al.*, *Eur. Phys. J.* **C72** (2012) 2022; LHCb collaboration, R. Aaij *et al.*, *JINST* **10** (2015) P10005; LHCb collaboration, R. Aaij *et al.*, *JINST* **11** (2016) P05010; LHCb collaboration, R. Aaij *et al.*, *Eur. Phys. J.* **C77** (2017) 238.
- [5] LHCb collaboration, R. Aaij *et al.*, *Phys. Lett.* **B774** (2017) 139.
- [6] A. Davis *et al.*, LHCb-PUB-2018-004, 2018.
- [7] R. Fleischer, *Nucl. Phys.* **B671** (2003) 459.
- [8] M. Pivk and F. R. Le Diberder, *Nucl. Instrum. Meth.* **A555** (2005) 356.
- [9] Particle Data Group, P. A. Zyla *et al.*, *Prog. Theor. Exp. Phys.* **2020** (2020) 083C01.
- [10] Heavy Flavor Averaging Group, Y. Amhis *et al.*, updated results and plots available at <https://hflav.web.cern.ch>.
- [11] M. Gronau and D. London, *Phys. Rev. Lett.* **65** (1990) 3381; M. Ciuchini *et al.*, *JHEP* **10** (2012) 29; R. Fleischer *et al.*, *JHEP* **03** (2017) 055.
- [12] LHCb collaboration, R. Aaij *et al.*, *Phys. Rev.* **D98** (2018) 032004.
- [13] V. Gligorov *et al.*, *Journal of Physics: Conference Series* **396** (2012) 022016.